Asian Journal of Civil Engineering
https://doi.org/10.1007/s42107-022-00560-7

RESEARCH

ANN-based model for predicting the axial load capacity of the cold-formed steel semi-oval hollow section column

Duy-Duan Nguyen[1] · Ngoc-Long Tran[1] · Trong-Ha Nguyen[1]

Received: 18 December 2022 / Accepted: 28 December 2022

Abstract
The cold-formed Steel Semi-oval Hollow Section (SSOHS) column is a new cross-section column and has been used a lot in construction projects. However, the design standards for steel structures in the world have not covered the cross-section classifications for the SSOHS columns in the design process. Therefore, the Axial Load Capacity (ALC) of the SSOHS column has been different between the design standards and experiments. This paper develops predictive tools (formula and graphical user interface) for calculating the ALC of the SSOHS columns based on an Artificial Neural Network (ANN) model. The ANN model has been developed with 219 datasets. The input parameters of the ANN model include the overall depth (*D*), the overall width (*B*), thickness (*t*) of the sections, and the length of the pin-ended columns (*L*). Meanwhile, the ALC of the SSOHS column is the output parameter of the ANN model. The predictive formula based on an ANN model is compared with three regression models and two existing formulas. The comparison results reveal that the performance of the ANN model outperform three regression models and two existing formulas through indicators: *R*-squared, *RMSE*, and *a20-index*. The sensitivity analyses of the input parameters to the ALC of the SSOHS column are also performed. Finally, a mathematical formula and graphical user interface program are developed to practically calculate the ALC of the SSOHS column.

Keywords Semi-oval hollow sections · Pin-ended columns · Cold-formed · ANN model · Predicted formula · Graphical user interface

Introduction

The Steel Semi-oval Hollow Section (SSOHS) is a new cross-section in the column, it is including a semi-circular flange, a flat flange, and two flat web plates as shown in Fig. 1. The SSOHS column has superior axial load capacity compared to square and circular cross-section columns (Zhu & Young, 2011, 2012). However, the design standards for steel structures in the world have not covered the SSOHS cross-section classification for the SSOHS column in the design process.

Recently, there were studies on the Axial Load Capacity (ALC) of the SSOHS column were carried out, but these studies have been still limited. On the other hand, the axial load capacity of the SSOHS column has been different between the theoretical and experimental. Reviewing some studies: In 2018 Chen and Young published the results of the experimental investigation and verification of the axial load capacity of the SSOHS column. In addition, this study has built a FEM data set to compare and modify the formula for the axial load capacity of the SSOHS column from the Direct Strength Method (DSM) (Chen & Young, 2018b). Meanwhile, Chen and Young (2018a) proposed some modifications to the DSM for the calculation of the axial load capacity of the SSOHS column after performing investigations of material behavior, cross-section, and residual stress. Checking some steel structure design standard codes such as ANSI/AISC-360: 2016, AISI-S100: 2016, AS/NZS-4600: 2005, and EN1993-1-1: 2005 (ANSI, 2016; AS/NZS-4600, 2005; Chen et al., 2016; Eurocode, 2005), it can be seen that the AISI S100-16 (Chen et al.,

✉ Trong-Ha Nguyen
trongha@vinhuni.edu.vn

Duy-Duan Nguyen
duan468@gmail.com

Ngoc-Long Tran
longtn@vinhuni.edu.vn

[1] Department of Civil Engineering, Vinh University, Vinh 461010, Vietnam

Published online: 11 February 2023

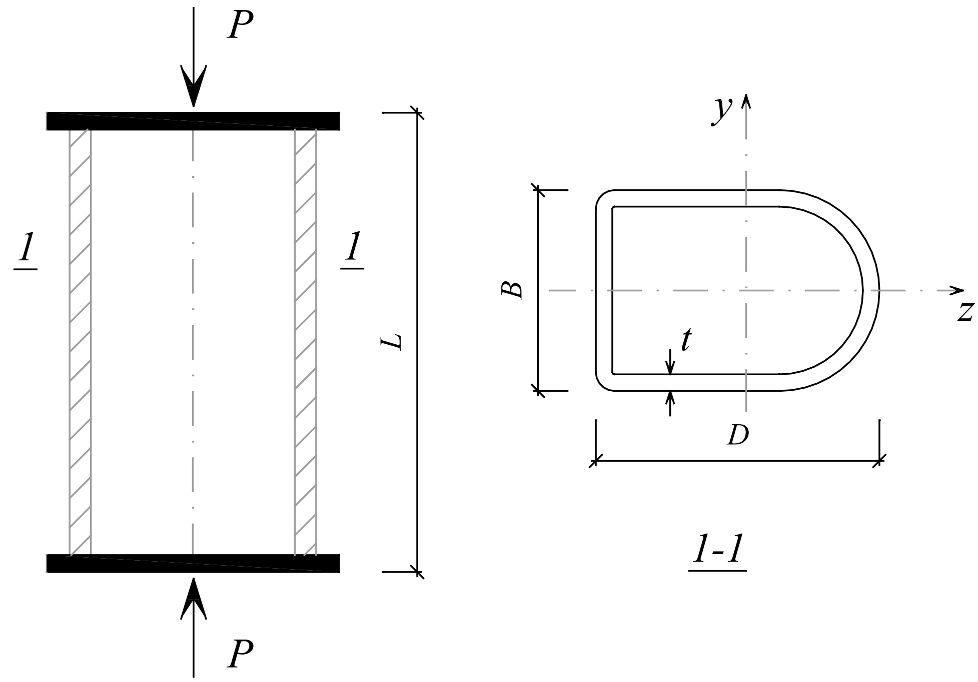

Fig. 1 The cross-sectional and geometry of the SSOHS column

Table 1 The statistical description of the input and output parameters

Input parameters	D (mm) (X_1)	B (mm) (X_2)	T (mm) (X_3)	L (mm) (X_4)	P(kN) (Output)
Minimum	93.00	60.00	2.00	200.00	176.00
Mean	301.51	174.88	7.13	2393.38	3445.07
Maximum	450.00	360.00	20.00	4000.00	16,250.50
Standard deviation (SD)	136.22	84.56	5.34	1115.52	3793.75
Coefficient of variation (CoV)	0.451	0.482	0.747	0.465	1.099

2016) has been the only standard used to calculate the design strength for any cross-sectional profile.

In the last few decades, with the development of IT, cloud computing, and big data, the application of artificial intelligence techniques has become popular in many areas of social life, especially in civil engineering (Kaveh & Bondarabady, 2004; Kaveh & Iranmanesh, 1998; Kaveh & Khalegi, 1998; Kaveh & Servati, 2001; Kaveh et al., 2008; Nguyen et al., 2022; Tran & Nguyen, 2022). Applying Artificial Neural Networks (ANNs) in the field of steel and reinforced concrete structures is a topic of interest to numerous researchers (Ahmed et al., 2019; Ho et al., 2022; Mai et al., 2022; Nguyen et al., 2021a, 2021b, 2021c; Rönnholm et al., 2005; Selvan et al., 2018; Tran & Kim, 2020; Tran et al., 2022; Vakhshouri & Nejadi, 2018; Yang et al., 1992; Zorlu et al., 2008). However, to the knowledge of the authors, there is not any research applying the ANN algorithm to predict the ALC of the SSOHS column.

This paper presents the predicted method of the ALC of the SSOHS column based on an ANN model. The ANN model has been developed with 219 datasets. Accordingly, the dataset was collected from the literature (Chen and Young, 2018a, b). The performance results of the ANN model were compared with that of three regression models and two existing formulas. Three statistical indicators for measuring the performance of predictive models were used. The sensitivity analysis of the input parameters to the ALC of the SSOHS column was also performed. Finally, practical tools, i.e., formula and graphical user interface program, were developed to calculate the ALC of the SSOHS column.

A dataset for the proposed ANN model

The ANN model has been developed with 219 datasets. The dataset was collected from the literature (Chen & Young, 2018a, b). Input parameters include the overall depth (D), the overall width (B), thickness (t) of the cross-sections, and the length of the pin-ended columns (L).

Meanwhile, the ALC of the SSOHS column is the output parameter of the ANN model. The statistical description of the input and output parameters is shown in Table 1. The probability distribution of data parameters is shown in Fig. 2.

The relationships between the four input parameters including the overall depth (D), the overall width

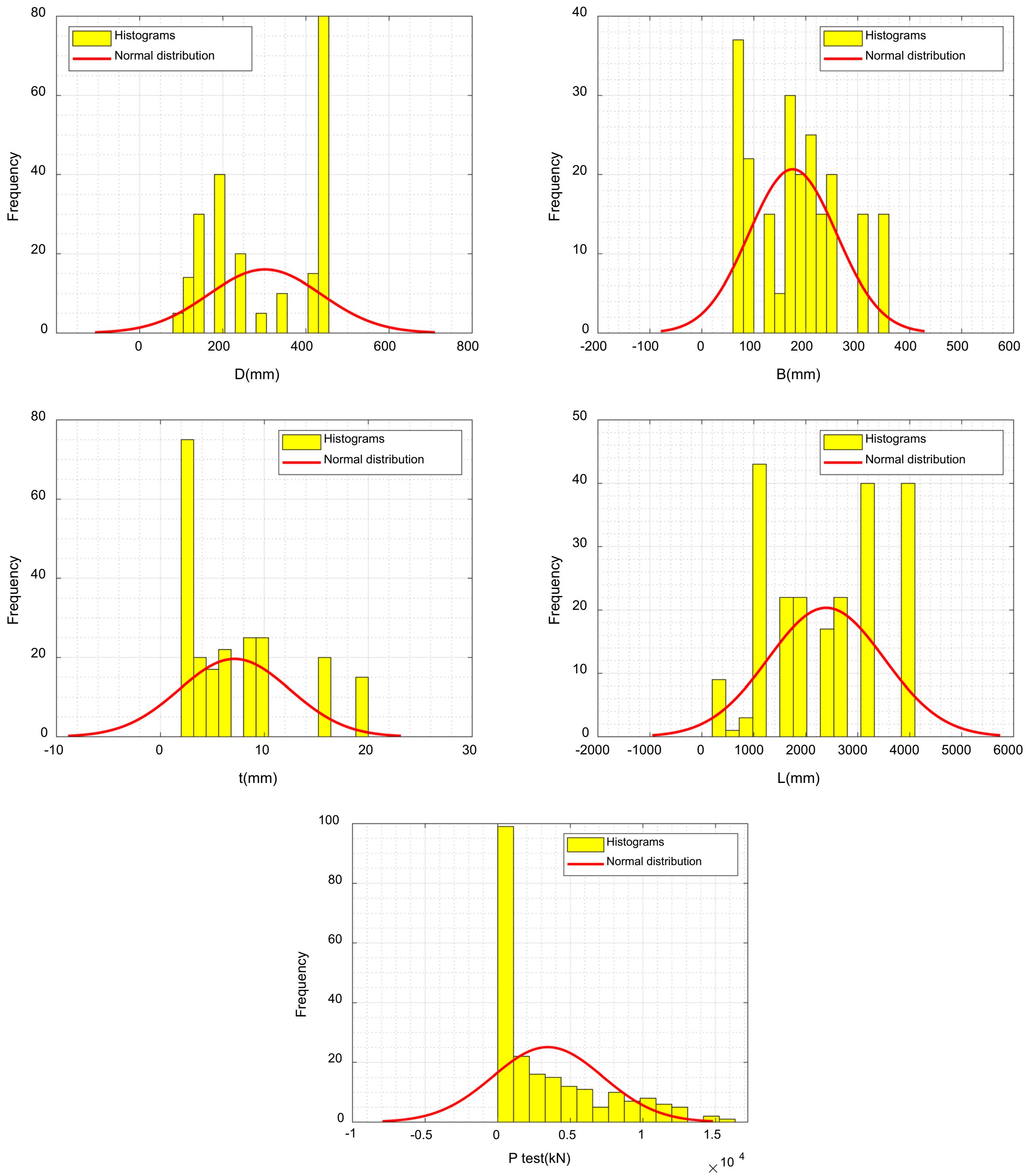

Fig. 2 The probability distribution of input and output parameters

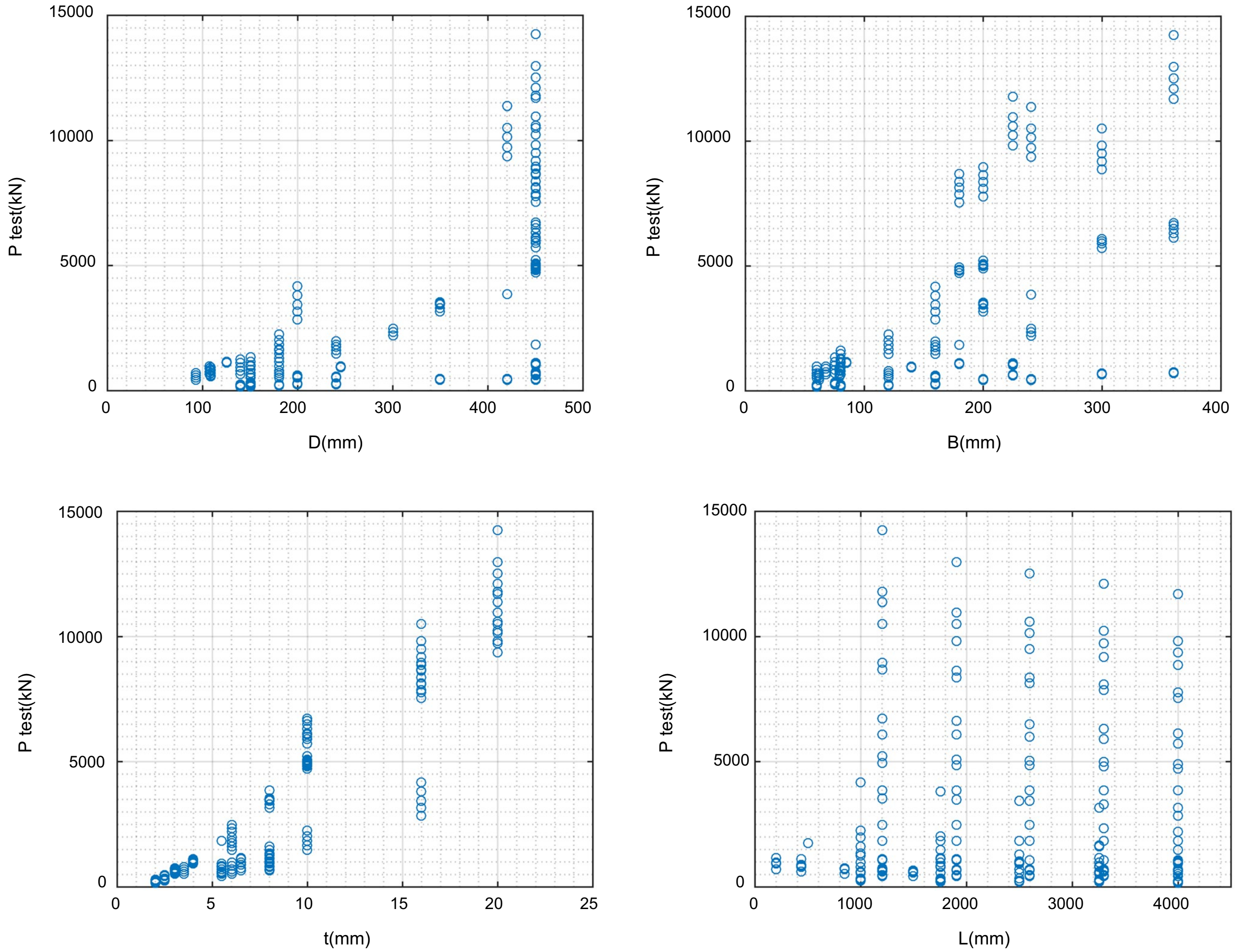

Fig. 3 Relationship between input and output parameters

(*B*), thickness (*t*) of the cross-sections, the length of the pin-ended columns (*L*), and the output parameter of the ALC of the SSOHS column are shown in Fig. 3. Figure 4 shows the correlation between input parameters and output parameters. It can be seen that the strongest correlation between the input parameters the overall depth (*D*) and the overall width (*B*) was 0.85, while the correlation between the thickness (*t*) and the length of the pin-ended columns (*L*) was 0.05. This confirms predicting the ALC of the SSOHS column with the collected data sets is even more meaningful.

Design code has been used for calculating the ALC of the SSOHS column

So far, determining the ALC of the SSOHS column was using the design codes AISI-S100 (2016) (Chen et al., 2016) or the expression proposed by Chen and Young (2018b). To demonstrate the performance of the ANN model, formulas specified by design codes AISI-S100 (2016) and the expression proposed by Chen and Young (2018b) were considered, as shown in Table 2.

Developed regression models

For the purpose of further confirming the performance of the ANN model in predicting the ALC of the SSOHS column, we used three regression models, which are First order (MLR1), Quadratic order (MLR2), and Quadratic with mixed terms (MLR3) based on the above datasets. The results obtained from the regression models are presented in Table 3.

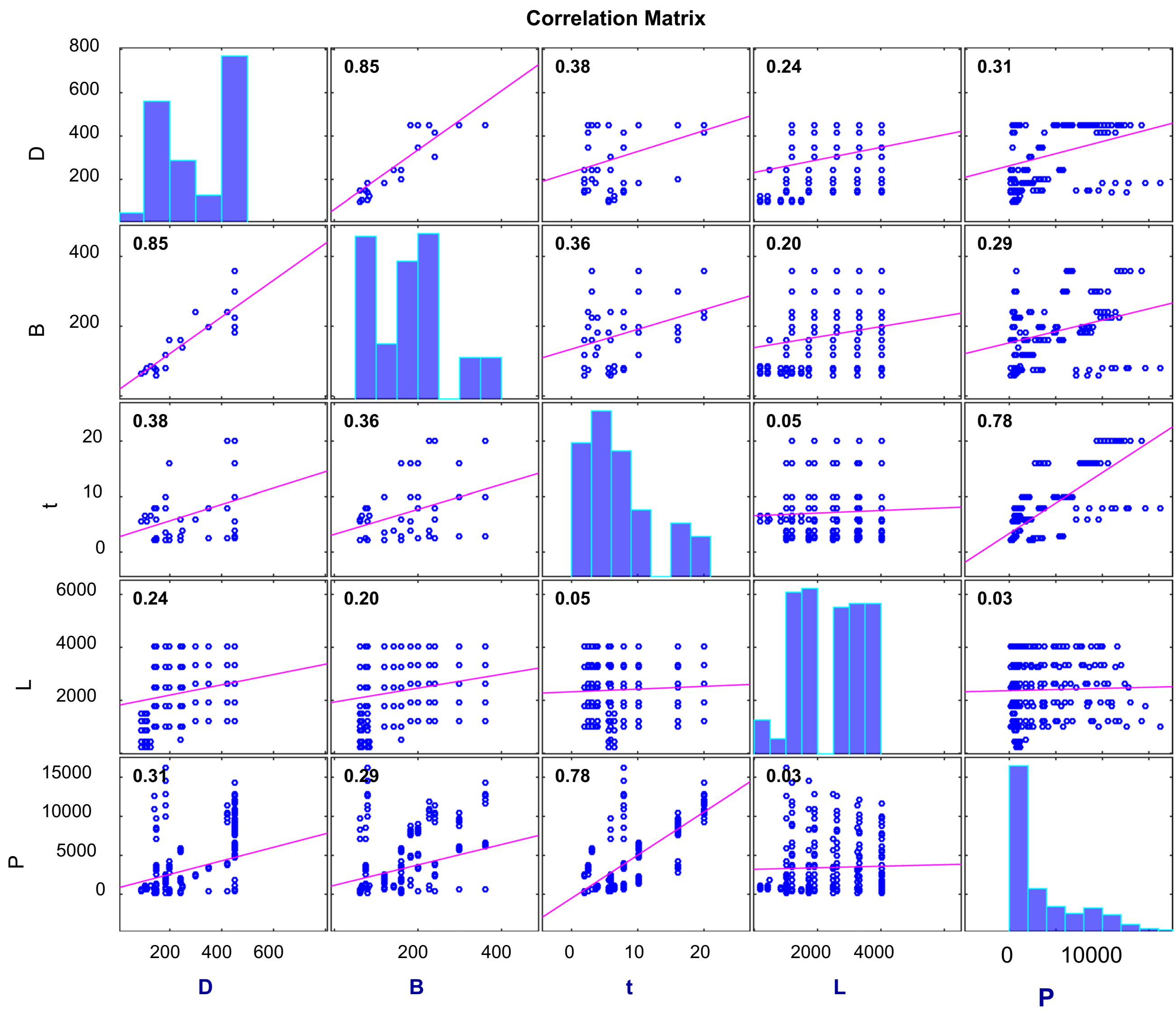

Fig. 4 Correlation between input and output parameters

The proposed ANN models

ANN model

Nowadays, ANN has been widely used in life and technology (Naser et al., 2021; Nguyen et al., 2021a, 2021b, 2021c; Patel & Mehta, 2018; Patil & Subbareddy, 2002; Tran et al., 2019, 2021; Zorlu et al., 2008). ANN is a computing system, which simulates the animal brain. The model contains connected units or nodes, so-called neurons. Basically, neurons are aggregated into layers. Typically, an ANN model has three layers, which are the input layer, hidden layer(s), and output layer, in which, these layers are connected through weights and biases. Different layers may perform different transformations on their inputs. Signals travel from the first layer (i.e., the input layer), to the last layer (i.e., the output layer). This study used a back-propagation (B-P) neural network and a Levenberg–Marquardt (L-M) algorithm. The mathematical representation of ANN model has the following form.

$$f : X \in R^D \rightarrow Y \in R^1$$

Table 2 Expression for determining the ALC of the SSOHS column

Reference	Formulas	
Chen and Young (2018b)	$P_{nl}^{*} = \begin{cases} 1.2P_y & \text{for } \lambda_l \le 0.472 \\ \left[1 - 0.168\left(\frac{P_{crl}}{P_y}\right)^{0.34}\right]\left(\frac{P_{crl}}{P_y}\right)^{0.34}P_y & \text{for } \lambda_l > 0.472 \end{cases}$ $\lambda_l \le 0.702$ with non-slender section $P_{ne}^{*} = \begin{cases} (1.2 - 0.6\lambda_c)P_y & \text{for } \lambda_c \le 0.5 \\ \left(\frac{0.877}{\lambda_c^2}\right)P_y & \text{for } \lambda_c > 0.5 \end{cases}$ $\lambda_l > 0.702$ with non-slender section $P_{ne}^{*} = \begin{cases} (KQ^{\lambda^R})P_{nl}^{*} & \text{for } \lambda_c \le 2.0 \\ \left(\frac{0.877}{\lambda_c^2}\right)P_y & \text{for } \lambda_c > 2.0 \end{cases}$ with, $K = 1.05 - 0.1\lambda_l$; $R = 2.5 - 0.025\lambda_l$; $Q = \left(\frac{0.21925}{K}\right)^{\frac{1}{2R}}$; $\lambda_l = \sqrt{\frac{P_y}{P_{crl}}}$; $\lambda_c = \sqrt{\frac{f_y}{f_{cre}}}$; $f_{cre} = \frac{\pi^2 E}{(L_e/r)^2}$;$P_y = f_y.A$ The modified DSM $(P_{DSM}^{*}) = \min(P_{nl}^{*}, P_{ne}^{*})$	(1)
AISI-S100 (2016) (Chen et al., 2016)	$P_{nl} = \begin{cases} P_{ne} & \text{for } \lambda_l \le 0.776 \\ \left[1 - 0.15\left(\frac{P_{crl}}{P_{ne}}\right)^{0.4}\right]\left(\frac{P_{crl}}{P_{ne}}\right)^{0.4}P_{ne} & \text{for } \lambda_l > 0.776 \end{cases}$ $\lambda_l = \sqrt{\frac{P_{ne}}{P_{crl}}}$; $P_{ne} = A_g F_n$ $F_n = \begin{cases} (0.658^{\lambda^2})F_y & \text{for } \lambda_c \le 1.50 \\ \left(\frac{0.877}{\lambda_c^2}\right)F_y & \text{for } \lambda_c > 1.50 \end{cases}$ With, $\lambda_c = \sqrt{\frac{F_y}{F_{cre}}}$; $F_{cre} = \frac{\pi^2 E}{(KL/r)^2}$ $P_{crl} = F_{crl}A_g = K\frac{\pi^2 E}{12(1-\mu^2)}\left(\frac{t}{w}\right)^2$ The design predicted by the DSM $P_{DSM}^{*} = P_{nl}$	(2)

$$f(X) = f_0\left(b_2 + W_2\left(f_h\left(b_1 + W_1X\right)\right)\right) \tag{3}$$

where $b_1$andW_1 represent the biases and weights; and f_h denotes the activation function of the hidden layer. Whereas $b_2$andW_2 are the biases and weight; and f_0 denote the activation function of the output layer.

The nonlinear activation function namely *tansig* is used for the hidden layer, while the linear function namely *purelin* has been used for the output layer (Nikbin et al., 2017). The expressions that represent the *tansig* and *purelin* activation function are shown in Eqs. (4) and (5) and Fig. 5.

$$\text{tansig}(x) = \frac{2}{(1 + epx(-2x))} - 1 \tag{4}$$

$$purelin(x) = x \tag{5}$$

According to Golafshani and Ashour (2016), during the training of the network, the input and output data must be normalized in the interval [− 1, 1]. The normalization equation is shown in Eq. (6).

$$X_n = 2 \times \frac{(X - X_{\min})}{(X_{\max} - X_{\min})} - 1 \tag{6}$$

The training process is continued until a convergence of the mean square error (*MSE*) obtained. The *MSE* is expressed by the following equation.

$$MSE = \min_{b_1, b_2, W_1, W_2} \frac{1}{n}\sum_{i=1}^{n} e_i^2 \tag{7}$$

where e_i is the error between the output and the experiment data; n is number of data samples.

Table 3 The coefficients of three regression models

Regression model	Regression function, y	Regression coefficients
First order (MLR1)	$a_0 + a_1X_1 + \cdots + a_4X_4$	$a_0 = -2784.89, a_1 = 3.12, a_2 = 6.58$ $a_3 = 514.75, a_4 = -0.12, R^2 = 0.9448.$
Quadratic order (MLR2)	$a_0 + a_1X_1 + \cdots + a_4X_4$ $+a_{11}X_1^2 + a_{22}X_2^2 + \cdots + a_{44}X_4^2$	$a_0 = -1829.94, a_1 = 19.55, a_2 = -18.30,$ $a_3 = 252.68, a_4 = -0.28, a_{11} = -0.02,$ $a_{22} = 0.05, a_{33} = 13.05, a_{44} = 1.0e-05,$ $R^2 = 0.9462.$
Quadratic with mixed terms (MLR3)	$a_0 + a_1X_1 + \cdots + a_4X_4$ $+a_{11}X_1^2 + a_{22}X_2^2 + \cdots + a_{44}X_4^2$ $+a_{12}X_1X_2 + \cdots + a_{34}X_3X_4$	$a_0 = -192.45, a_1 = -0.18, a_2 = 0.23$ $a_3 = 35.50, a_4 = 0.10, a_{11} = -0.01, a_{22} = -0.10,$ $a_{33} = -7.40, a_{44} = 1.0e-7,$ $a_{12} = 0.01, a_{13} = 1.43, a_{14} = 1.0e-5,$ $a_{23} = 0.82, a_{24} = 1.0e-5, a_{34} = -0.04,$ $R^2 = 0.9986.$

Evaluation of optimal ANN model

For obtaining the best ANN model, various ratios of training data should be used. Also, different numbers of neurons in hidden layers need to be considered. To evaluate the optimal model, three indicators: R^2, *RMSE*, and *a20-index* were utilized (Zorlu et al., 2008). The equations for determining the R^2, *RMSE*, and *a20-index*, respectively, are as follows.

$$R^2 = 1 - \frac{\sum_{i=1}^{n}(y_i - \hat{y}_i)^2}{\sum_{i=1}^{n}(y_i - \overline{y})^2} \tag{8}$$

$$RMSE = \sqrt{\frac{1}{n}\sum_{i=1}^{n}(y_i - \hat{y}_i)^2} \tag{9}$$

$$a20 - index = \frac{m20}{n} \tag{10}$$

where y_i is the *i*th value of the experimental data; $\hat{y}_i$ is the *i*th value of the predicted value of ANN model; $\overline{y}$ is the average value of the experiment; n is the number of samples; *m20* is the number of samples with the ratio of the experimental value to the predicted value between 0.8–1.0.

For the current study, a total of 120 ANN models were tested with six training ratios (0.6, 0.65, 0.70, 0.75, 0.8, 0.85). While the number of neurons in the hidden layer was varied from 1 to 20. The optimal model was the model with the highest ranking (i.e., largest *R*-squared and *a20-index*, smallest *RMSE*). The ranking results of 120 models are shown in Fig. 6. It can be seen that the best-performing models have training, testing, and validation ratios (0.7, 0.15, 0.15), respectively. And 13 hidden layer neurons as shown in Fig. 7.

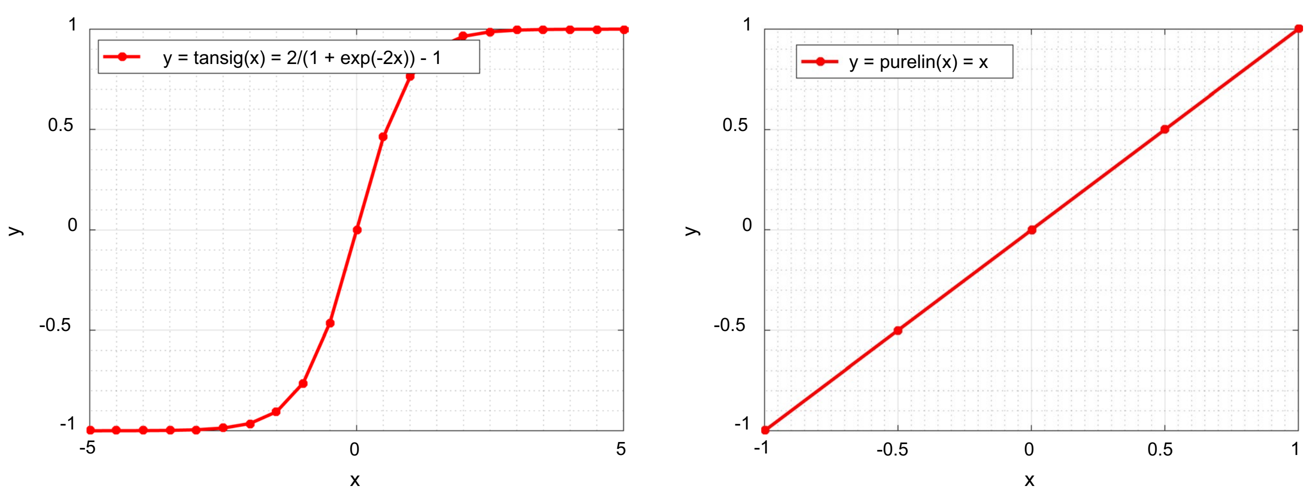

Fig. 5 Activation function *tansig*(*x*) (left) and *purelin*(*x*) (right)

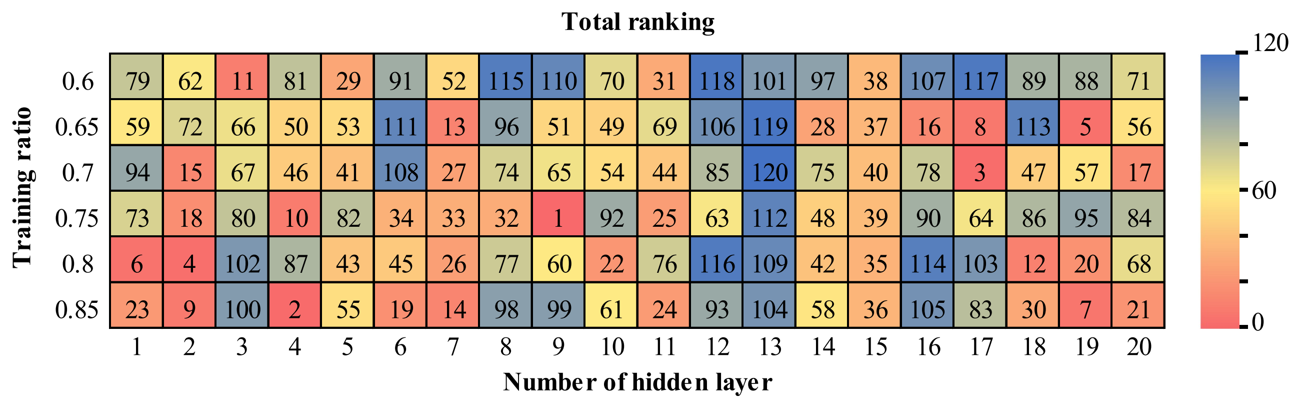

Fig. 6 Ranking matrix of 120 proposed ANN structures

Performance of ANN models with the datasets

The training results of the ANN model with the input datasets are shown in Fig. 8. It can be seen that the training stops at the 22th epoch at $MSE = 9.89e{-}05$. This confirms that the proposed ANN model has been trained very well with the input data.

Figures 9, 10 and 11 show the ALC of the SSOHS column obtained from the ANN model and the test datasets including all data, training data, testing data, and validation data. Can be seen that the error frequency converges at zero and is mostly smaller than 0.035. Once again confirm that the proposed ANN model structure is reliable for predicting the ALC of the SSOHS column.

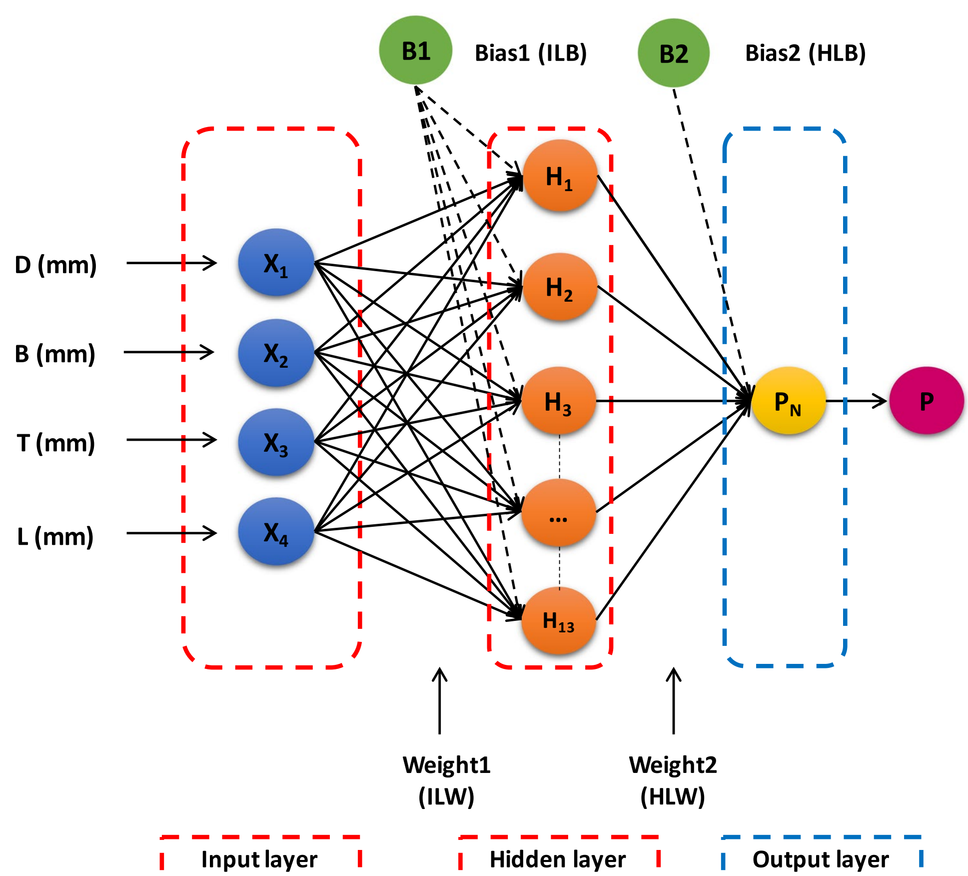

Fig. 7 The proposed ANN model structure

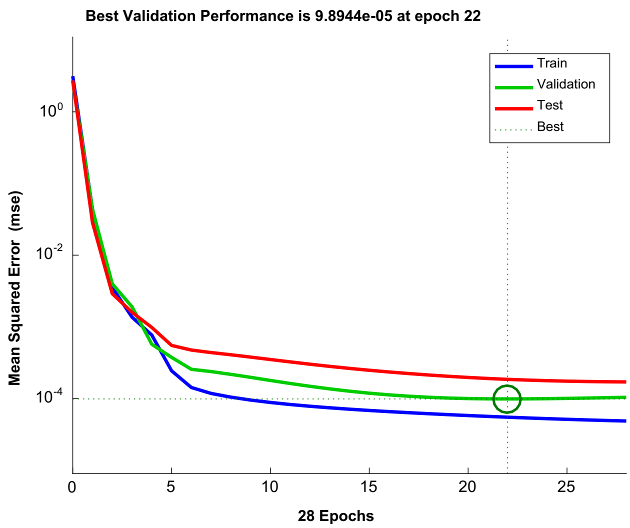

Fig. 8 Performance of proposed ANN model

Comparison between the proposed ANN model and existing formulas

The prediction a formula based on an ANN model was compared with three regression models (First order—MLR1, Quadratic order—MLR2, and Quadratic with mixed terms—MLR3) and two existing formulas (AISI-S100 (2016) (Chen et al., 2016) and the expression proposed by Chen and Young (2018a). The comparison result of the performance of the ANN model to predict the ALC of the SSOHS column with three regression models and two existing formulas based on the *R*-squared, *RMSE*, *MAPE*, and Pearson correlation coefficient (*r*) was presented in Fig. 12 and Table 4.

Figure 14 shows the difference of the *R*-squared, *RMSE*, *MAPE*, and Pearson correlation coefficient (*r*) of the different models. However, the proposed ANN model outperforms, the smallest *RMSE*, *MAPE* indexes while the

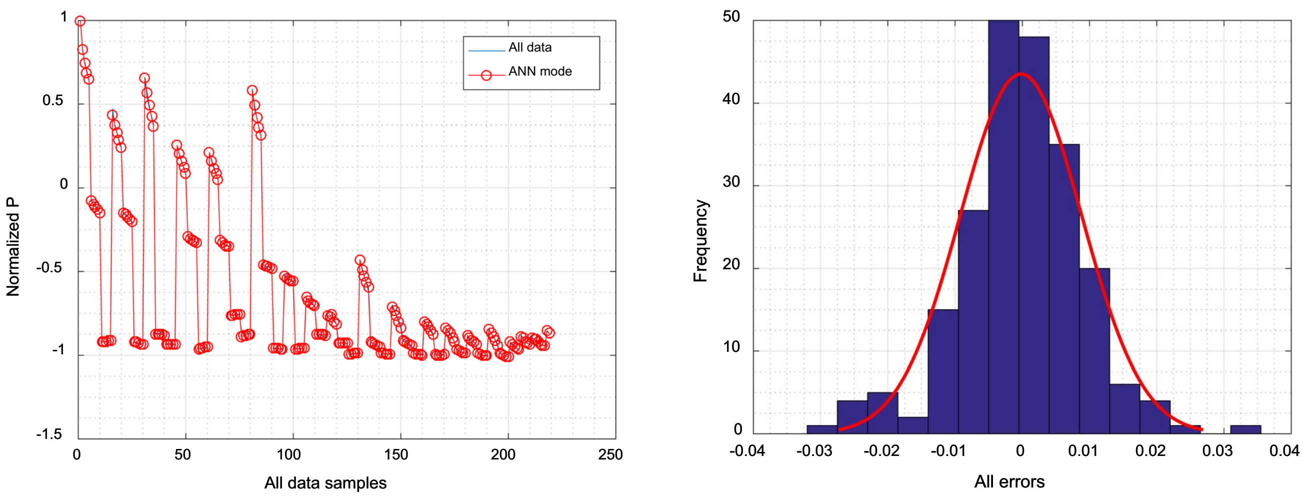

Fig. 9 Performance of All data

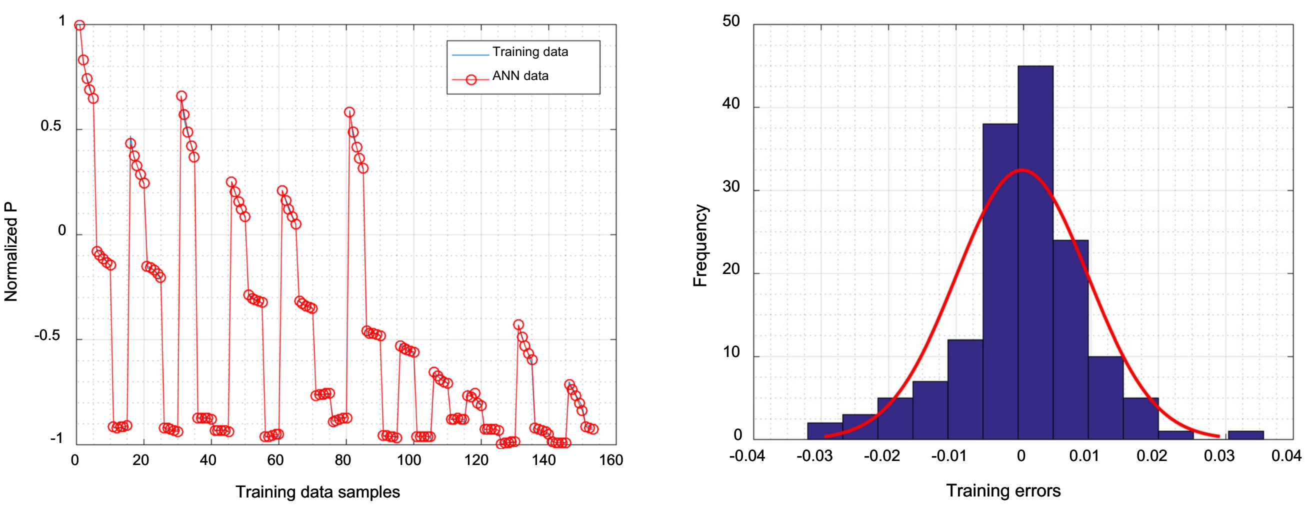

Fig. 10 Performance of the training data

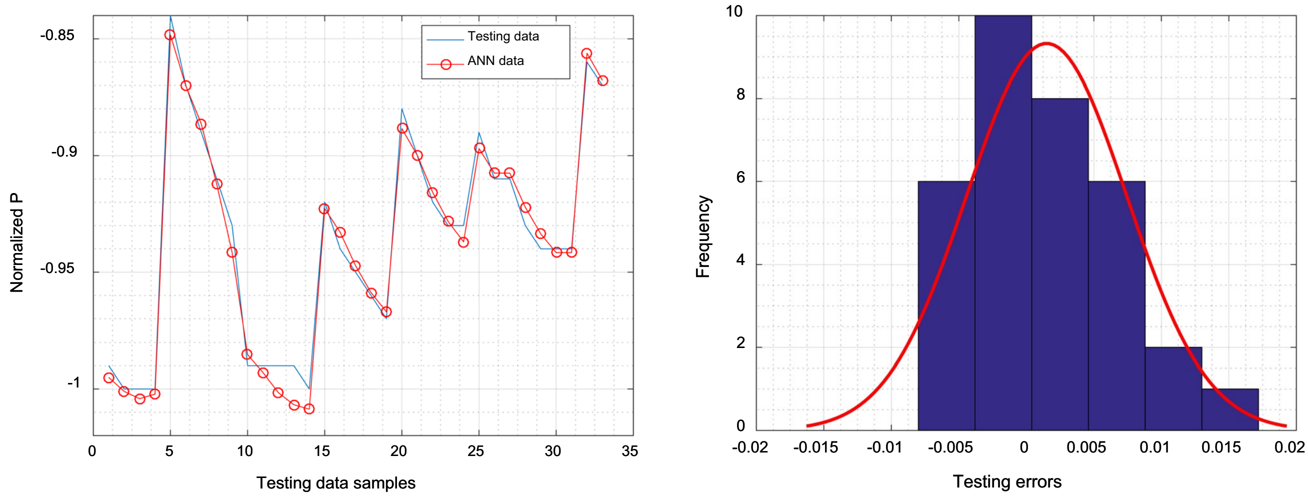

Fig. 11 Performance of the testing data

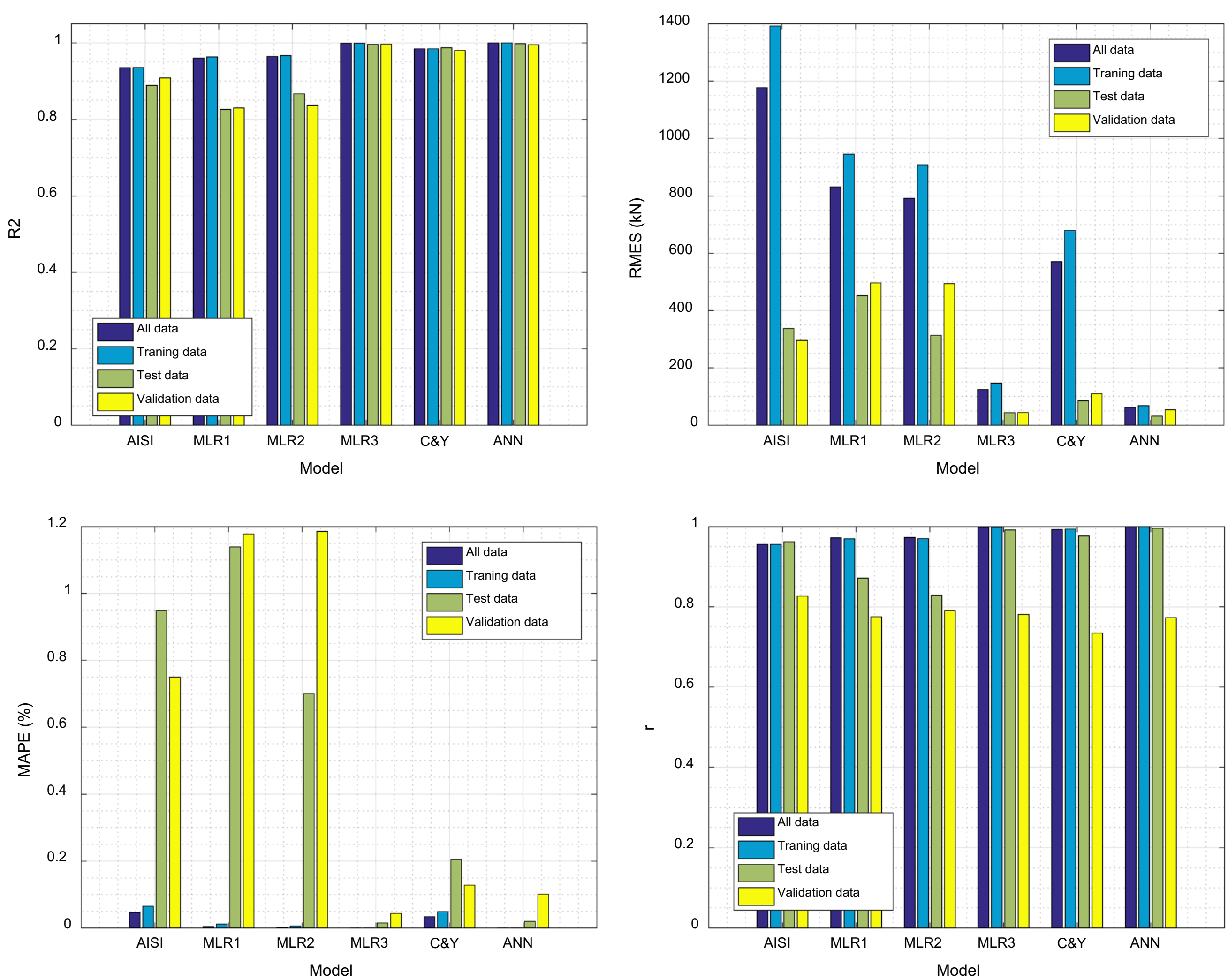

Fig. 12 Statistical results of the predictive models

Table 4 Performance of different predictive models

Predicted model	R^2	RMSE(kN)	MAPE(%)	r	$P_{\text{prediction}}/P_{\text{Test}}$				
					Min	Max	SD	Mean	COV
AISI-S100 (2016) (Chen et al., 2016)	0.9137	1176.905	0.0465	0.9559	0.1984	1.9669	0.4734	0.7634	0.6139
Chen and Young (2018a, 2018b)	0.9857	571.024	0.0339	0.9928	0.6930	3.0704	0.6324	1.4319	0.4393
MLR1	0.9448	831.842	0.0039	0.9720	0.0630	3.2305	0.5932	1.2740	0.4627
MLR2	0.9462	791.968	0.0012	0.9728	0.1088	3.9422	0.6650	1.2547	0.5265
MLR3	0.9986	124.756	0.0001	0.9993	0.0960	1.3309	0.1562	0.9816	0.1576
ANN model	0.9996	61.833	0.0001	0.9998	0.6061	1.2860	0.0919	0.9931	0.0917

Table 5 Coefficients for formulation (11)

i	h_i	c_{io}	c_{i1}	c_{i2}	c_{i3}	c_{i4}
0	0.3656					
1	0.0271	2.5149	0.0960	−2.2318	−0.4123	1.7187
2	−0.2515	−2.2446	1.1335	0.3315	−2.4424	−0.0642
3	−0.4833	2.7420	−0.8580	−0.0956	−1.4865	0.3825
4	−0.0887	1.4028	−1.0597	−1.3898	−2.5042	−0.3967
5	−0.0671	0.8466	−1.4945	0.0742	−0.8591	−0.5840
6	0.1743	−0.7059	1.3489	0.5655	−0.9924	0.1258
7	−0.0145	0.4132	0.4951	1.3809	−0.4869	2.2319
8	0.5083	−0.1978	−0.0763	0.2869	0.8851	−0.1627
9	0.0299	1.0169	0.9286	−1.8839	0.6058	−1.0941
10	−0.1905	−1.2064	−1.9231	0.3176	1.3781	0.1023
11	−0.0258	−1.8770	−0.7883	−1.1975	−1.2928	−1.7768
12	−0.4352	2.8659	0.9236	−1.4506	−0.9770	1.5943
13	−0.1044	2.9864	0.8462	−1.7417	−1.6454	−0.7403

R-squared and Pearson correlation coefficient (r) has reached the maximum value (close to 1.0).

Table 4 shows the R-squared, *RMSE*, *MAPE*, Pearson correlation coefficient (r), and probability statistics (Minimum, Maximum, Mean, St.D, CoV) of the ratio predicted/dataset. It can be seen the mean value of the ANN model is close to 1.0. Once again confirm that the proposed ANN model structure is reliable for predicting the ALC of the SSOHS column.

The predictive formula for ALC of SSOHS columns

The proposed ANN model predicting the ALC of the SSOHS column has been presented. This study has been proposed an expression to determine the ALC of the SSOHS column using the activation function, weight, and biases vector with the normalized Eq. (6), which is expressed as follows.

$$P = 7027.60\left(P_N + 1\right) + 176.0 \tag{11}$$

where the coefficients 7027.60 and 176.0 are half the value of the maximum and minimum ALC difference, and the minimum ALC value of the input datasets, respectively. P_N is the normalized ALC values determined by the following expression.

$$P_N = h_0 + \sum_{i=1}^{13} h_i H_i$$

$$H_i = tanh\left(c_{i0} + c_{i1}X_1 + c_{i2}X_2 + c_{i3}X_3 + c_{i4}X_4\right) \tag{12}$$

In which, the h_0, h_i và $c_{i0}, \ldots, c_{i4}$ are obtained from the ANN model, and collected in Table 5.

Sensitivity analysis of input parameters on the ALC of the SSOHS column

The effects of the input parameters on the ALC of the SSOHS column will be helped designers and managers to assess which parameters are significant and important for the bearing capacity of the structure. The input parameter has been changed from minimum (L) to maximum (H). At the time to assess X_i parameter, the remaining parameters have been also changed from minimum (L) to maximum (H) value. All databases are shown in Table 6.

The effect of the input parameter on the ALC of the SSOHS column was presented in this section. The four

Table 6 The databases of the input parameters

Input parameters	L	ML	M	MH	H
D (mm) (X_1)	93.00	197.26	301.51	375.76	450.00
B (mm) (X_2)	60.00	117.44	174.88	267.44	360.00
t (mm) (X_3)	2.00	4.57	7.13	13.57	20.00
L (mm) (X_4)	200.00	1296.69	2393.38	3196.69	4000.00

L low, *LM* middle low, *M* medium, *MH* middle high, *H* high

input parameters were changed from the low value (*L*) to the high value (*H*), while the other input parameters were changed in turn corresponding to the data set given in Table 6. The results of the sensitivity analysis are shown in Fig. 13.

Figure 13 shows the effect of the input parameters on the ALC of the SSOHS column. It can be seen that the ALC of the SSOHS column value tended to increase with

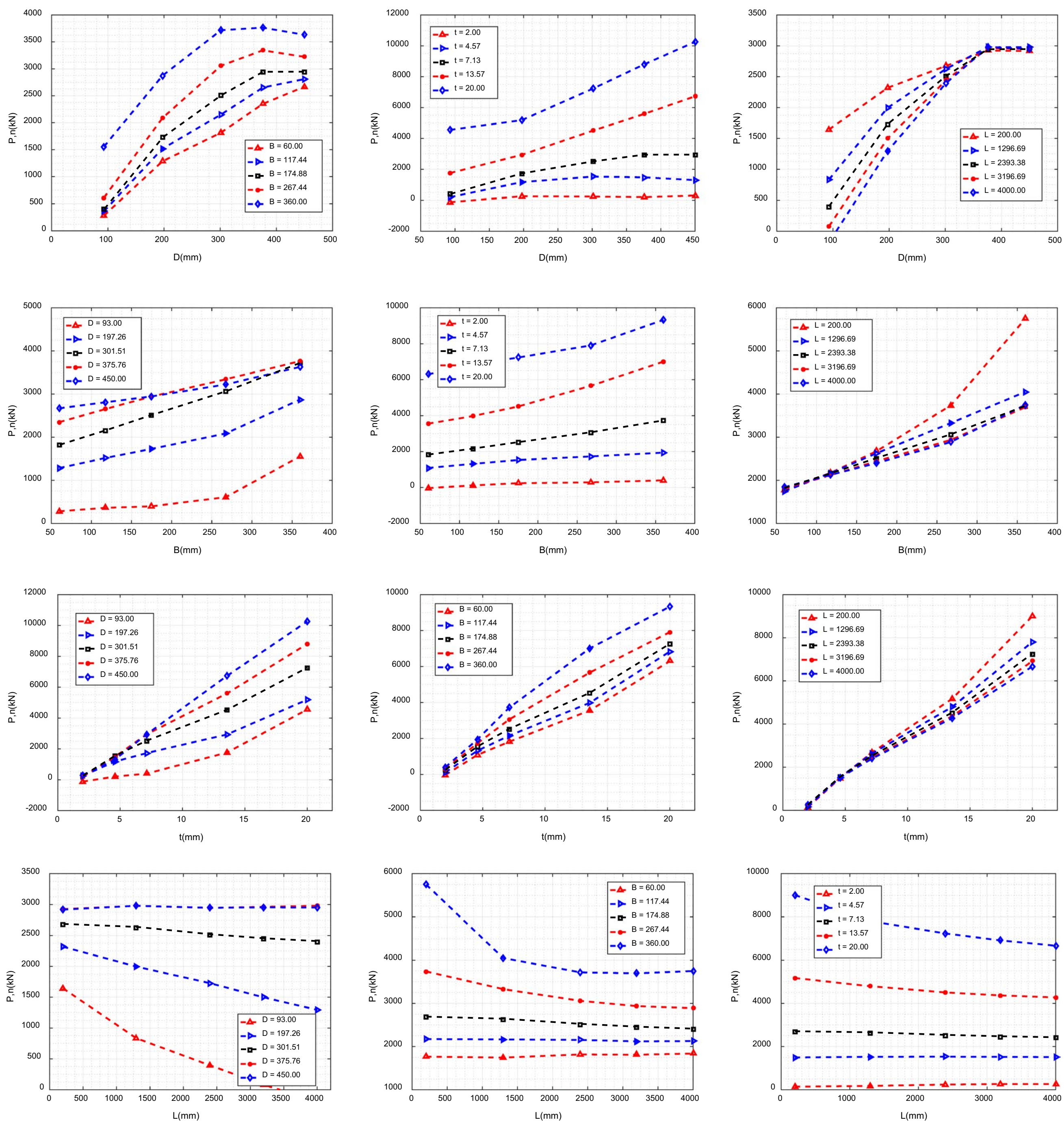

Fig. 13 Effects of input parameters on the ALC of the SSOHS column

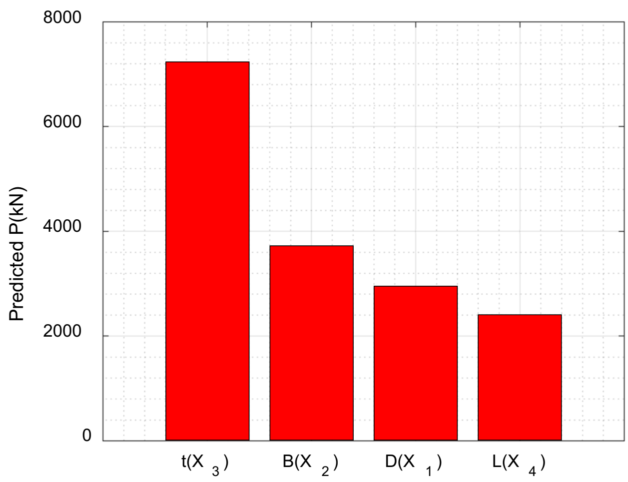

Fig. 14 Sensitivity of input parameters on the ALC of the SSOHS column

the increase of the overall depth D (i.e. X_1) and the overall width (B) (i.e. X_2), and the thickness (t) (i.e. X_3) of the cross-section. Meanwhile, the ALC of the SSOHS column value was reduced with the length of the pin-ended columns (L) (i.e. X_4) being increased.

Figure 14 shows the effect of the input parameters on the ALC of the SSOHS column. The ALC of the SSOHS column value corresponds to the maximum value of each variable. The maximum sensitivity value belongs to the thickness (t). Thus, increasing thickness (t) gives the most efficient for the ALC of the SSOHS column.

Graphical user interface program

The graphical user interface (GUI) program was developed using MATLAB. It is easy to calculate the ALC of the SSOHS column for designers and managers as shown in Fig. 15. The four input parameters include the overall depth (D), the overall width (B), thickness (t) of the cross-sections, the length of the pin-ended columns (L). This tool is convenient and it is provided freely. To determine the ALC of the SSOHS column, we put all the input variables and click to "Start Predict". This GUI tool was developed using the proposed ANN model, the accuracy of the prediction has been verified and demonstrated in the previous section.

It should be noted that the ANN model only predicts results within the range of input data (i.e., from the

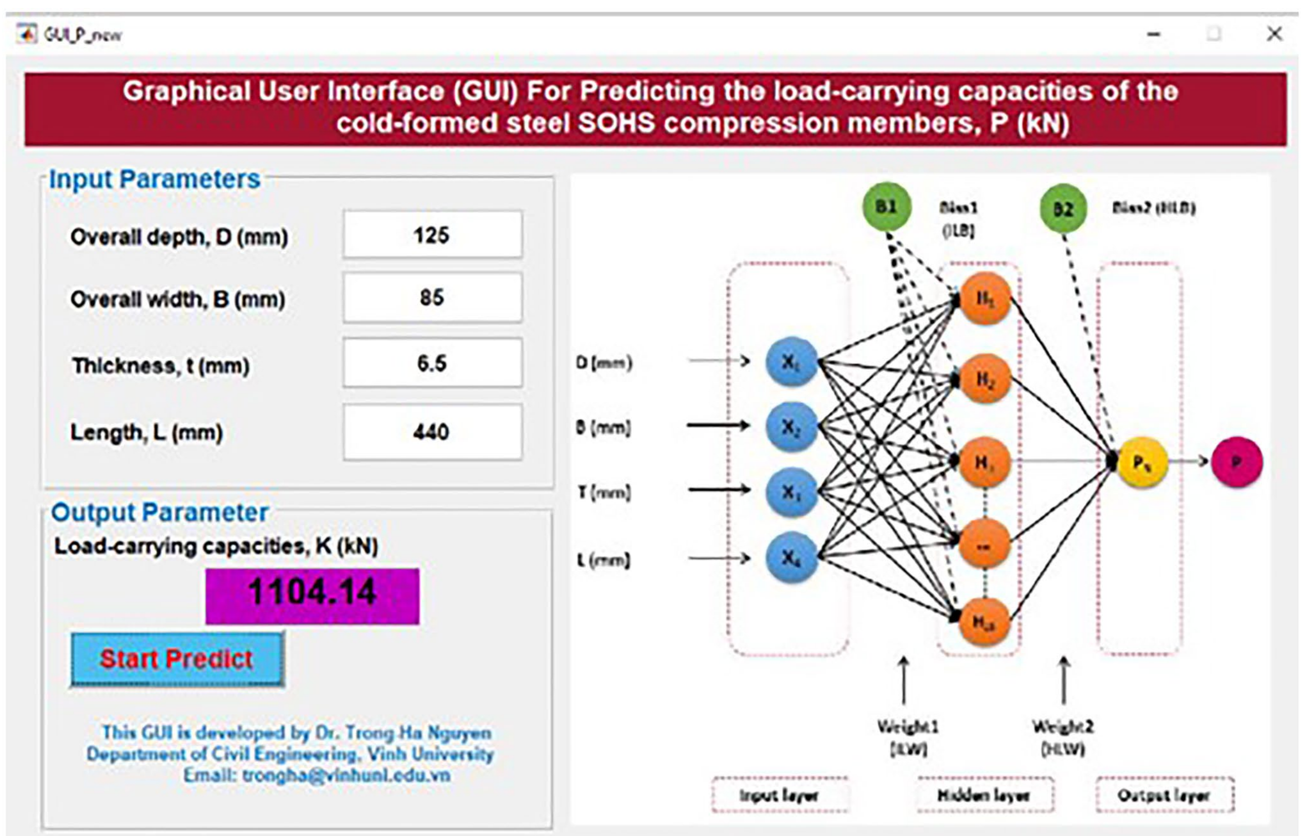

Fig. 15 Graphical user interface programs

minimum to the maximum). For enlarging the boundary of the model a wide range of collected data samples should be considered.

Conclusions

This paper developed an ANN model to predict the ALC of the SSOHS column based on 219 experimental data. The training process of the ANN model shows that the prediction results were reliable. Some important conclusions are drawn.

- The study uses 219 datasets for the proposed ANN model. Based on a comparison with other existing models, the proposed ANN model shows that the prediction results are more reliable.
- A formulation to determine the ALC of the SSOHS column is proposed based on the training results of the ANN model.
- The developed GUI program is convenient for designers and managers in practical calculations.
- The effects of input parameters on the ALC of the SSOHS column are assessed. Thickness (t) gives the most efficient for the ALC of the SSOHS column.

Supplementary Information The online version contains supplementary material available at https://doi.org/10.1007/s42107-022-00560-7.

Author contributions D-DN: Methodology, formal analysis, writing—original draft, writing—review and editing; N-LT: Data curation, visualization, validation; T-HN: Conceptualization, software, writing—original draft, writing—review and editing, supervision.

Funding No funding was used in this study.

Data availability The data used to support the findings of this study are included in the article.

Declarations

Conflict of interest The authors declare that they have no known competing financial interests or personal relationships that could have appeared to influence the work reported in this paper.

References

Ahmed, A., Elkatatny, S., Ali, A., Mahmoud, M., & Abdulraheem, A. (2019). New model for pore pressure prediction while drilling using artificial neural networks. *Arabian Journal for Science and Engineering, 44*, 6079–6088. https://doi.org/10.1007/s13369-018-3574-7

ANSI, A. (2016). Specification for structural steel buildings. ANSI/AISC 360-16.

AS/NZS-4600. (2005). AS/NZS 4600:2005 cold-formed steel structure.

Chen, H., Brockenbrough, R., & Haws, R. (2016). AISI standards developed and updated in 2015 and 2016.

Chen, M.-T., & Young, B. (2018a). Cross-sectional behavior of cold-formed steel semi-oval hollow sections. *Engineering Structures, 177*, 318–330.

Chen, M.-T., & Young, B. (2018b). Experimental and numerical investigation on cold-formed steel semi-oval hollow section compression members. *Journal of Constructional Steel Research, 151*, 174–184.

Eurocode, C. (2005). 3: Design of steel structures—Part 1-1: General rules and rules for buildings. CEN, Brussels: European Committee for Standardization

Golafshani, E. M., & Ashour, A. (2016). A feasibility study of BBP for predicting shear capacity of FRP reinforced concrete beams without stirrups. *Advances in Engineering Software, 97*, 29–39.

Ho, V.-C., Nguyen, T.-H., Nguyen, T.-Q., & Nguyen, D.-D. (2022). Application of neural networks for the estimation of the shear strength of circular RC columns. *Engineering, Technology & Applied Science Research, 12*, 9409–9413.

Kaveh, A., & Bondarabady, H. R. (2004). Wavefront reduction using graphs, neural networks and genetic algorithm. *International Journal for Numerical Methods in Engineering, 60*, 1803–1815.

Kaveh, A., Gholipour, Y., & Rahami, H. (2008). Optimal design of transmission towers using genetic algorithm and neural networks. *International Journal of Space Structures, 23*, 1–19.

Kaveh, A., & Iranmanesh, A. (1998). Comparative study of backpropagation and improved counterpropagation neural nets in structural analysis and optimization. *International Journal of Space Structures, 13*, 177–185.

Kaveh, A., & Khalegi, A. (1998). Prediction of strength for concrete specimens using artificial neural networks. In: *Advances in engineering computational technology* (pp. 165–171).

Kaveh, A., & Servati, H. (2001). Design of double layer grids using backpropagation neural networks. *Computers & Structures, 79*, 1561–1568.

Mai, S. H., Tran, V.-L., Nguyen, D.-D., Nguyen, V. T., & Thai, D.-K. (2022). Patch loading resistance prediction of steel plate girders using a deep artificial neural network and an interior-point algorithm. *Steel and Composite Structures, 45*, 159.

Naser, M., Thai, S., & Thai, H.-T. (2021). Evaluating structural response of concrete-filled steel tubular columns through machine learning. *Journal of Building Engineering, 34*, 101888. https://doi.org/10.1016/j.jobe.2020.101888

Nguyen, D.-D., Tran, V.-L., Ha, D.-H., Nguyen, V.-Q., & Lee, T.-H. (2021a). *A machine learning-based formulation for predicting shear capacity of squat flanged RC walls* (pp. 1734–1747). Elsevier.

Nguyen, T.-H., Tran, N.-L., & Nguyen, D.-D. (2021b). Prediction of axial compression capacity of cold-formed steel oval hollow section columns using ANN and ANFIS models. *International Journal of Steel Structures*. https://doi.org/10.1007/s13296-021-00557-z

Nguyen, T.-H., Tran, N.-L., & Nguyen, D.-D. (2021c). Prediction of critical buckling load of web tapered I-section steel columns using artificial neural networks. *International Journal of Steel Structures*. https://doi.org/10.1007/s13296-021-00498-7

Nguyen, V.-Q., Tran, V.-L., Nguyen, D.-D., Sadiq, S., & Park, D. (2022). Novel hybrid MFO-XGBoost model for predicting the racking ratio of the rectangular tunnels subjected to seismic loading. *Transportation Geotechnics, 37*, 100878.

Nikbin, I. M., Rahimi, S., & Allahyari, H. (2017). A new empirical formula for prediction of fracture energy of concrete based on the artificial neural network. *Engineering Fracture Mechanics, 186*, 466–482. https://doi.org/10.1016/j.engfracmech.2017.11.010

Patel, V. M., & Mehta, H. B. (2018). Thermal performance prediction models for a pulsating heat pipe using artificial neural network

(ANN) and regression/correlation analysis (RCA). *Sādhanā, 43*, 1–16. https://doi.org/10.1007/s12046-018-0954-3

Patil, S. B., & Subbareddy, N. (2002). Neural network based system for script identification in Indian documents. *Sadhana, 27*, 83–97. https://doi.org/10.1007/BF02703314

Rönnholm, M., Arve, K., Eränen, K., Klingstedt, F., Salmi, T., & Saxén, H. (2005). ANN modeling applied to NO X reduction with octane. ANN future in personal vehicles. *Adaptive and natural computing algorithms* (pp. 100–103). Springer. https://doi.org/10.1007/3-211-27389-1_24

Selvan, S. S., Pandian, P. S., Subathira, A., & Saravanan, S. (2018). Comparison of response surface methodology (RSM) and artificial neural network (ANN) in optimization of *Aegle marmelos* oil extraction for biodiesel production. *Arabian Journal for Science and Engineering, 43*, 6119–6131. https://doi.org/10.1007/s13369-018-3272-5

Tran, N.-L., Nguyen, D.-D., & Nguyen, T.-H. (2022). Prediction of speed limit of cars moving on corroded steel girder bridges using artificial neural networks. *Sādhanā, 47*, 1–14.

Tran, N.-L., Nguyen, T.-H., Phan, V.-T., & Nguyen, D.-D. (2021). A machine learning-based model for predicting atmospheric corrosion rate of carbon steel. *Advances in Materials Science and Engineering, 2021*, 1–25.

Tran, V.-L., & Kim, S.-E. (2020). Efficiency of three advanced data-driven models for predicting axial compression capacity of CFDST columns. *Thin-Walled Structures, 152*, 106744. https://doi.org/10.1016/j.tws.2020.106744

Tran, V.-L., & Nguyen, D.-D. (2022). Novel hybrid WOA-GBM model for patch loading resistance prediction of longitudinally stiffened steel plate girders. *Thin-Walled Structures, 177*, 109424.

Tran, V.-L., Thai, D.-K., & Kim, S.-E. (2019). Application of ANN in predicting ACC of SCFST column. *Composite Structures, 228*, 111332. https://doi.org/10.1016/j.compstruct.2019.111332

Vakhshouri, B., & Nejadi, S. (2018). Prediction of compressive strength of self-compacting concrete by ANFIS models. *Neurocomputing, 280*, 13–22. https://doi.org/10.1016/j.neucom.2017.09.099

Yang, H., Akiyama, T., & Sasaki, T. (1992). A neural network approach to the identification of real time origin-destination flows from traffic counts.

Zhu, J.-H., & Young, B. (2011). Cold-formed-steel oval hollow sections under axial compression. *Journal of Structural Engineering, 137*, 719–727.

Zhu, J.-H., & Young, B. (2012). Design of cold-formed steel oval hollow section columns. *Journal of Constructional Steel Research, 71*, 26–37.

Zorlu, K., Gokceoglu, C., Ocakoglu, F., Nefeslioglu, H., & Acikalin, S. (2008). Prediction of uniaxial compressive strength of sandstones using petrography-based models. *Engineering Geology, 96*, 141–158. https://doi.org/10.1016/j.enggeo.2007.10.009